Lumsden, P. J., Yamamoto, K. T., Nagatani, A., & Furuya, M. (1985) *Plant Cell Physiol. 26*, 1313–1322.
Margulies, L., & Stockburger, M. (1979) *J. Am. Chem. Soc. 101*, 743–744.
McMichael, R. W., Jr., & Lagarias, J. C. (1990) *Biochemistry 29*, 3872–3878.
Moon, D.-K., Jeen, G.-S., & Song, P.-S. (1985) *Photochem. Photobiol. 42*, 633–641.
Rospendowski, B. N., Farrens, D. L., Cotton, T. M., & Song, P.-S. (1989) *FEBS Lett. 258*, 1–4.
Rudiger, W. (1987) in *Phytochrome and Photoregulation in Plants* (Furuya, M., Ed.) pp 127–138, Academic Press, Tokyo.
Rudiger, W., Thummler, F., Cmiel, E., & Schneider, S. (1983) *Proc. Natl. Acad. Sci. U.S.A. 80*, 6244–6248.
Rudiger, W., Eilfeld, P., & Thummuler, F. (1985) in *Optical Properties and Structure of Tetrapyrroles* (Blauer, G., & Sund, H., Eds.) pp 349–366, W. de Gryter & Co., Berlin.
Sakmar, T. P., Franke, R. R., & Khorana, H. G. (1989) *Proc. Natl. Acad. Sci. U.S.A. 86*, 8309–8313.
Sarker, H. K., & Song, P.-S. (1981) *Biochemistry 20*, 4315–4320.
Sawatzki, J., Fischer, R., Scheer, H., & Siebert, F. (1990) *Proc. Natl. Acad. Sci. U.S.A. 87*, 5903–5906.
Schirmer, T., Bode, W., & Huber, R. (1987) *J. Mol. Biol. 196*, 677–695.
Schuster, I. I., & Roberts, J. D. (1979) *J. Org. Chem. 44*, 3864–3867.
Siebert, F., Grimm, R., Rudiger, W., Schmidt, G., & Scheer, H. (1990) *Eur. J. Biochem. 194*, 921–928.
Spiro, T. G., Ed. (1987) *Biological Applications of Raman Spectroscopy*, Wiley, New York.
Srinivasan, P. R., & Lichter, R. L. (1977) *J. Magn. Reson. 28*, 227–234.
Thummler, F., & Rudiger, W. (1983) *Tetrahedron 39*, 1943–1951.
Thummler, F., Eilfeld, P., Rudiger, W., Moon, D.-K., & Song, P.-S. (1985) *Z. Naturforsch 40C*, 215–218.
Tokutomi, S., Yamamoto, K. T., Miyoshi, Y., & Furuya, M., (1982) *Photochem. Photobiol. 35*, 431–433.
Tokutomi, S., Inoue, Y., Sato, N., Yamamoto, K. T., & Furuya, M. (1986) *Plant Cell Physiol. 27*, 765–773.
Tokutomi, S., Yamamoto, K. T., & Furuya, M. (1988a) *Photochem. Photobiol. 47*, 439–445.
Tokutomi, S., Kataoka, M., Sakai, J., Nakasako, M., Tokunaga, F., Tasumi, M., & Furuya, M. (1988b) *Biochim. Biophys. Acta 953*, 297–305.
Tokutomi, S., Nakasako, M., Sakai, J., Kataoka, M., Yamamoto, K. T., Wada, M., Tokunaga, F., & Furuya, M. (1989) *FEBS Lett. 247*, 139–142.
Tokutomi, S., Mizutani, Y., Anni, H., & Kitagawa, T. (1990) *FEBS Lett. 269*, 341–344.
Vierstra, R. D., & Quail, P. H. (1982) *Planta 156*, 158–165.
Vierstra, R. D., & Quail, P. H. (1983) *Plant Physiol. 72*, 264–267.
Witanowski, M., Stefaniak, L., Szymanski, S., & Januszewski, H. (1977) *J. Magn. Reson. 28*, 217–226.
Wong, Y.-S., Cheng, H.-C., Walsh, D. A., & Lagarias, J. C. (1986) *J. Biol. Chem. 261*, 12089–12097.
Yamamoto, K. T. (1987) in *Phytochrome and Photoregulation in Plants* (Furuya, M., Ed.) pp 63–82, Academic Press, Tokyo.
Yamamoto, K. T., & Tokutomi, S. (1989) *Photochem. Photobiol. 50*, 113–120.

Rate and Mechanism of the Assembly of Tropomyosin with Actin Filaments†

Christiane Weigt,‡ Albrecht Wegner,*,‡ and M. H. J. Koch§

Institute of Physiological Chemistry, Ruhr University, D W-4630 Bochum, Federal Republic of Germany, and European Molecular Biology Laboratory (EMBL), Deutsches Elektronensynchrotron (DESY), Notkestr. 85, D W-2000 Hamburg, Federal Republic of Germany

Received April 9, 1991; Revised Manuscript Received July 3, 1991

ABSTRACT: The rate of assembly of tropomyosin with actin filaments was measured by stopped-flow experiments. Binding of tropomyosin to actin filaments was followed by the change of the fluorescence intensity of a (dimethylamino)naphthalene label covalently linked to tropomyosin and by synchrotron radiation X-ray solution scattering. Under the experimental conditions (2 mM $MgCl_2$, 100 mM KCl, pH 7.5, 25 °C) and at the protein concentrations used (2.5–24 μM actin, 0.2–3.4 μM tropomyosin) the half-life time of assembly of tropomyosin with actin filaments was found to be less than 1 s. The results were analyzed quantitatively by a model in which tropomyosin initially binds to isolated sites. Further tropomyosin molecules bind contiguously to bound tropomyosin along the actin filaments. Good agreement between the experimental and theoretical time course of assembly was obtained by assuming a fast preequilibrium between free and isolatedly bound tropomyosin.

Tropomyosin is a long rodlike molecule associated with actin filaments (Bailey, 1948; Martonosi, 1962; Laki et al., 1962). In non-muscle cells both free actin filaments and actin filaments covered with tropomyosin have been detected. In cultured human lung cells tropomyosin has been found to associate with newly formed actin filaments after a lag time of a few minutes (Lazarides, 1976). Tropomyosin regulates the assembly and stability of actin filaments and the actin-activated myosin ATPase (Ebashi et al., 1969; Spudich et al., 1972; Jahnke & Heilmeyer, 1983). Further, it stabilizes actin filaments against spontaneous fragmentation or fragmentation by severing proteins and retards binding of monomers to the

† This study was supported by the Bundesminister fuer Forschung und Technologie (Grant 05 432LAB 5) and by the Deutsche Forschungsgemeinschaft (Grant We 808/7).
* To whom correspondence should be addressed.
‡ Ruhr University.
§ European Molecular Biology Laboratory.

0006-2960/91/0430-10700$02.50/0

ends of actin filaments (Wegner, 1982; Hitchcock-DeGregori et al., 1988; Hinssen, 1981; Bernstein & Bamburg, 1982; Fattoum et al., 1983; Ishikawa et al., 1989; Bonder & Mooseker, 1983; Keiser & Wegner, 1985; Lal & Korn, 1986; Wegner & Ruhnau, 1988). Tropomyosin may also have other functions in modulating actin filament assembly by competing with actin-binding proteins such as α-actinin and filamin, which bind to the same actin sites as tropomyosin (Drabikowski et al., 1968; Maruyama et al., 1978; Zeece et al., 1979).

A number of tropomyosin isoforms have been isolated and characterized (Bailey, 1948; Cohen & Cohen, 1972; Tanaka & Hatano, 1972; Fine et al., 1973; Cotê et al., 1978; Bretscher & Weber, 1978; Der Terrossian et al., 1981; Giometti & Anderson, 1984; Keiser & Wegner, 1985; Hosoya et al., 1989; Liu & Bretscher, 1989). The muscle isoforms tend to be longer than the non-muscle isoforms. The muscle isoforms cover seven actin filament subunits in one strand of the double-helical actin filament while non-muscle tropomyosins are only six subunits long (Huxley & Brown, 1967; Hartshorne & Pyun, 1971, Bremel & Weber, 1972; McLachlan et al., 1975; Parry 1974; Cohen & Cohen, 1972; Fine et al., 1973; Schloss & Goldman, 1980). Muscle isoforms have a higher affinity for actin filaments than non-muscle isoforms (Tanaka & Oosawa, 1971; Fine et al., 1973; Wegner, 1979, Kobayashi et al., 1982; Cotê & Smillie, 1981; Keiser & Wegner, 1985). Both in the free and in the actin-bound state tropomyosin molecules can form end-to-end contacts (Casper et al., 1969; Cohen & Cohen, 1972; Huxley & Brown, 1967), giving rise to cooperative assembly of tropomyosin with actin filaments. Tropomyosin binds with low affinity to isolated binding sites on actin filaments but with high affinity to sites contiguous to actin-bound tropomyosin molecules (Wegner, 1979; Yang et al., 1979, Walsh & Wegner, 1980; Szczesna et al., 1989).

Several studies on the equilibrium of binding of tropomyosin to actin filaments have been reported (Wegner, 1979, 1980; Walsh & Wegner, 1980). Recently, the kinetics of binding of tropomyosin to actin filaments adjacent to actin-bound tropomyosin molecules has been analyzed in terms of rate constants of contiguous binding of tropomyosin (Wegner & Ruhnau, 1988). Little is known, however, about the overall rate of assembly of tropomyosin with actin filaments, which includes initial binding of tropomyosin to isolated and subsequent binding to contiguous sites. As this reaction is a fundamental process in the formation of microfilaments, we measured the time course and interpreted the measurements in terms of a model of assembly of tropomyosin with actin filaments.

Materials and Methods

Preparation of Actin. Rabbit skeletal muscle actin was prepared according to the method of Rees and Young (1967). The protein was applied to a Sephacryl S-200 column (2.5 × 90 cm) equilibrated with ATP buffer (0.5 mM ATP, 0.2 mM $CaCl_2$, 200 mg/L NaN_3, 5 mM triethanolamine hydrochloride, pH 7.5). The concentration of actin was determined by the method of Lowry (Lowry et al., 1951) and photometrically at 290 nm using an absorption coefficient of 24900 M^{-1} cm^{-1} (Wegner, 1976).

Preparation of Tropomyosin. Rabbit skeletal muscle tropomyosin–troponin complex was extracted from the residue remaining after preparation of actin (Spudich & Watt, 1971). Tropomyosin was separated from troponin and purified by hydroxyapatite chromatography (Eisenberg & Kielley, 1974). The fractions containing α,α-tropomyosin were pooled and used for the experiments. Tropomyosin was labeled with 6-acryloyl-2-(dimethylamino)naphthalene (acrylodan) according to Clark and Burtnick (1988). The labeled tropomyosin was dialyzed against 5 mM triethanolamine hydrochloride, pH 7.5. The extent of labeling was determined by measuring the concentrations of acrylodan and tropomyosin in the sample. Acrylodan was determined photometrically using an absorption coefficient of 12900 M^{-1} cm^{-1} at 360 nm (Prendergast et al., 1983). The concentration of tropomyosin was determined by the Lowry method (Lowry et al., 1951) or by absorption at 276 nm using an absorption coefficient of 24500 M^{-1} cm^{-1} (Wegner, 1979). Between 1 and 1.3 acrylodan groups were found to be bound per tropomyosin chain.

Time-Resolved Synchrotron X-ray Scattering. Solution scattering patterns were recorded on the X33 double-focusing mirror–monochromator camera of the EMBL in HASYLAB (Koch & Bordas, 1983) on the storage ring DORIS of the Deutsches Elektronen Synchrotron (DESY) at Hamburg. A quadrant detector with delay line readout (Gabriel & Dauvergne, 1982) was used with the standard data acquisition system and data evaluation software (Boulin et al., 1986, 1988). For the stopped-flow experiments a modified version of the device described by Berthet-Colominas et al. (1984) was used. In each shot, equal volumes (100 μL) of a solution of actin filaments (48 μM) and tropomyosin (6.7 μM) were mixed in about 75 ms. Tropomyosin was dissolved in ATP buffer containing additional 2 mM $MgCl_2$ and 100 mM KCl. Actin filaments were prepared by mixing ATP buffer, a 20 mM $MgCl_2$ solution, a 1 M KCl solution, and monomeric actin to final concentrations of 2 mM $MgCl_2$, 100 mM KCl, 0.18 mM $CaCl_2$, 0.45 mM ATP, 4.5 mM triethanolamine hydrochloride, pH 7.5, 2.7 mM NaN_3, and the desired concentration of actin. Scattering patterns were recorded in 256 time frames of 10 or 50 ms, and the results of about 100 shots were averaged. Similarly, in control experiments buffer was mixed with itself or with the actin solution. The relative mass per unit length and the radius of gyration of the cross-section were evaluated by extrapolation to $s = 0$ of $\log (s\, I(s))$ versus s^2 in the range $0.05 < s < 0.1$ nm^{-1}. $I(s)$ is the scattering corresponding to the scattering vector $s = (2 \sin \Theta)/\lambda$, where 2Θ is the scattering angle and λ the wavelength (0.15 nm).

Fluorescence Stopped Flow. Binding of tropomyosin to actin filaments was followed by the increase of the fluorescence intensity of bound fluorescently labeled tropomyosin compared to that of free labeled tropomyosin (Clark & Burtnick, 1988). For fluorescence stopped-flow experiments the solutions of labeled tropomyosin and of actin filaments were prepared as described for the X-ray stopped-flow measurements. The time course of assembly of tropomyosin with actin filaments was measured at 25 °C using a fluorescence stopped-flow device consisting of two syringes with equal cross-sections. The fluorescence was measured using a Perkin-Elmer LS-3 fluorometer with an excitation wavelength of 365 nm and an emission wavelength of 518 nm. The result of a typical fluorescence experiment is depicted in the top panel of Figure 1. The initial delay of about 0.7 s results from the dead time of the electronics and from the mixing. The signal to noise ratio was improved by averaging 26 measurements (Figure 1, bottom panel).

Light Scattering. The applicability of the fluorescence signal was tested by measuring light scattering and fluorescence of the same samples; 1-mL solutions of different tropomyosin concentrations in ATP buffer and 100 mM KCl were mixed with 1 mL of ATP buffer containing 6 mM $MgCl_2$ and 200 mM KCl. Before mixing in light-scattering cells, all solutions were centrifuged at 100000g for 1 h to remove dust. The

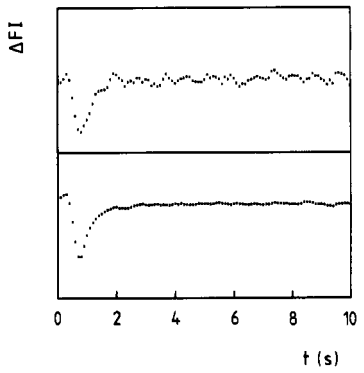

FIGURE 1: Fluorescence increase (ΔFI) during assembly of tropomyosin (0.7 μM) with actin filaments (2.5 μM) measured using a fluorescence stopped-flow apparatus: (top) trace of a single experiment; (bottom) average of 26 experiments.

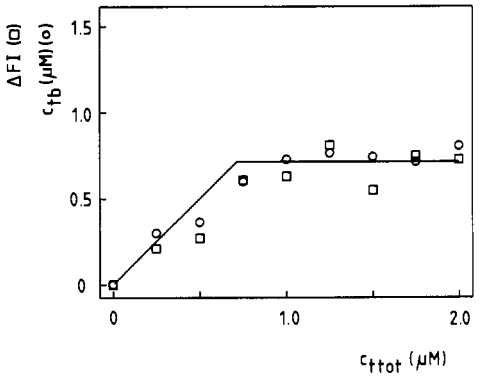

FIGURE 2: Binding of tropomyosin to actin filaments measured by light scattering and fluorescence of acrylodan-labeled tropomyosin: c_{ttot}, total tropomyosin concentration; c_{tb}, concentration of actin-bound tropomyosin; total actin concentration, 5 μM; ○, concentration of bound tropomyosin measured by light scattering; □, increase of the fluorescence intensity of tropomyosin (arbitrary units); —, curve calculated for irreversible binding of tropomyosin.

scattering intensities of the tropomyosin samples were measured at an angle of 90° at 518 nm using a Jobin Yvon 3D fluorometer, and the fluorescence intensities were subsequently determined. A total of 1 mL of monomeric actin was added to a final concentration of 5 μM. The samples were polymerized by incubation for 12 h at 25 °C. The scattering and fluorescence of the tropomyosin actin filaments were measured.

The ratio of the scattering intensities of long rodlike actin filaments (R_a) and of actin filaments to which tropomyosin is bound (R_t) has been shown to be given by (Wegner, 1979)

$$\frac{R_t}{R_a} = \frac{(C_a + C_t)^2}{C_a^2} \quad \text{or} \quad C_t = C_a\sqrt{(R_t/R_a)} - 1 \qquad (1)$$

C_a is the weight concentration of polymeric actin; C_t is the weight concentration of tropomyosin bound to actin filaments. For calculation of molar concentrations the molecular masses of actin and tropomyosin were assumed to be 42.300 and 65.400 kDa, respectively (Elzinga et al., 1973; Hodges et al., 1972). Figure 2 illustrates that the difference between the fluorescence intensities of pure labeled tropomyosin and actin-bound labeled tropomyosin is proportional to the concentration of bound tropomyosin. This allows the use of fluorescence to determine actin-bound tropomyosin.

RESULTS

Size and Shape of Actin Filaments and Actin–Tropomyosin Filaments. The changes of the solution scattering pattern which result from binding of tropomyosin to actin filaments

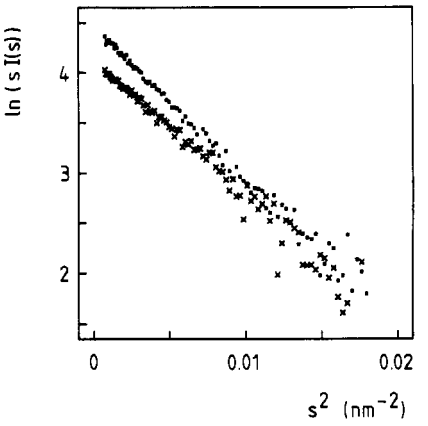

FIGURE 3: Solution X-ray scattering pattern; ×, actin filaments (24 μM); ■, actin–tropomyosin filaments (24 μM actin, 3.4 μM tropomyosin.

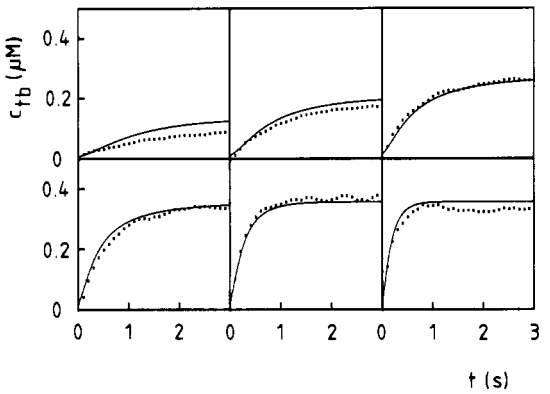

FIGURE 4: Time course of assembly of various concentrations of tropomyosin with 2.5 μM actin filaments: c_{tb}, concentration of actin-bound tropomyosin. Total tropomyosin concentrations: (top panels) left 0.2 μM, middle 0.3 μM, right 0.4 μM; (bottom panels) left 0.6 μM, middle 0.8 μM, right 1.0 μM. The lines represent curves calculated for a fast preequilibrium between free tropomyosin and isolatedly bound tropomyosin (equilibrium constant $K_N = 2.6 \times 10^4$ M^{-1}) and a rate constant for contiguous binding of tropomyosin $k^+ = 38 \times 10^6$ M^{-1} s^{-1} (numerical integration of eqs 3–5 and 7).

are illustrated in Figure 3. The radius of gyration of the cross-section of actin filaments is 2.6 ± 0.1 nm as reported earlier (Sayers et al., 1985; Matsudaira et al., 1987). Upon mixing of tropomyosin with actin filaments this value increases to up to 3.0 ± 0.1 nm (Figure 3). The apparent mass per unit length increases by 30–40% except at a molar ratio of tropomyosin to actin between 0.14 and 0.2 where a doubling of the mass per unit length was found. A simple estimate of the increase in mass per unit length and cross-section assuming that one tropomyosin binds to seven actin subunits would give an increase of about 20% of the mass per unit length and of 10% for the radius of gyration of the cross-section. This estimate based on solid cylinders represents a lower limit for the effect. Side by side aggregation of two filaments would double the mass per unit length but increase the radius of gyration of the cross-section to about 4.5 nm. Since the value of the radius of gyration is independent of the concentration determination, it is also more precise and suggests that binding of tropomyosin to actin filaments and not side by side aggregation of filaments is the most likely cause for the observed changes in the solution scattering patterns.

Rate of Assembly of Tropomyosin with Actin Filaments. The time course of assembly of tropomyosin with actin filaments was measured after mixing the proteins in a stopped-flow apparatus. In Figures 4 and 5 the time courses of the assembly of different tropomyosin concentrations (0.2–1.4 μM)

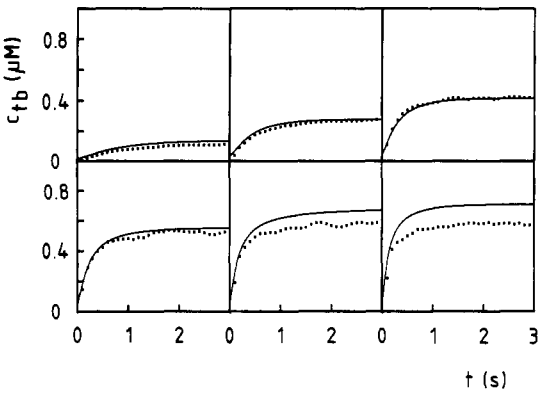

FIGURE 5: Time course of assembly of various concentrations of tropomyosin with 5 μM actin filaments: c_{tb}, concentration of actin-bound tropomyosin. Total tropomyosin concentrations: (top panels) left 0.2 μM, middle 0.4 μM, right 0.6 μM; (bottom panels) left 0.8 μM, middle 1.0 μM, right 1.2 μM. The lines represent curves calculated for a fast preequilibrium between free tropomyosin and isolatedly bound tropomyosin (equilibrium constant $K_N = 2.6 \times 10^4$ M^{-1}) and a rate constant of contiguous binding of tropomyosin $k^+ = 38 \times 10^6$ M^{-1} s^{-1} (numerical integration of eqs 3–5 and 7).

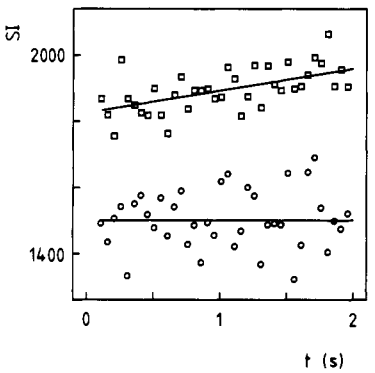

FIGURE 6: Time course of the integrated scattering (SI) in the range $0.05 < s < 0.1$ nm^{-1}; □, 24 μM actin filaments mixed with 3.4 μM tropomyosin; ○, 24 μM actin filaments mixed with buffer. Note that the scattering intensity of free tropomyosin is negligible.

with 2.5 or 5 μM actin are depicted. The results of the time-resolved X-ray scattering experiments are shown in Figure 6. At low concentrations of actin filaments (2.5–5 μM) and tropomyosin (<1.4 μM) the half-life time of assembly was in the range from 0.2 to 0.6 s. At the higher concentrations used for X-ray scattering (24 μM actin filaments, 3.4 μM tropomyosin) most of the assembly reaction has taken place during the mixing time (50–100 ms) and the half-life time was in the range of 50 ms or below. These measurements give an estimate on the rate of the assembly of tropomyosin with actin filaments. In the next sections the measured time course of formation of tropomyosin actin filaments will be interpreted by a simple assembly mechanism.

Model for Binding of Tropomyosin to Actin Filaments. A reaction scheme for the binding of tropomyosin to actin filaments based on observations reported in the literature is depicted in Figure 7.

(a) Tropomyosin molecules bind along the two grooves on both sites of actin filaments, thereby covering seven subunits in one strand of the double-helical actin filament (O'Brien et al., 1971).

(b) Tropomyosin molecules tend to form end to end contacts when they bind to actin filaments. A single tropomyosin molecule binds to actin filaments with lower affinity than a contiguous tropomyosin molecule as a result of the contacts formed not only with the actin filament but also with an adjacent tropomyosin molecule (Wegner, 1979).

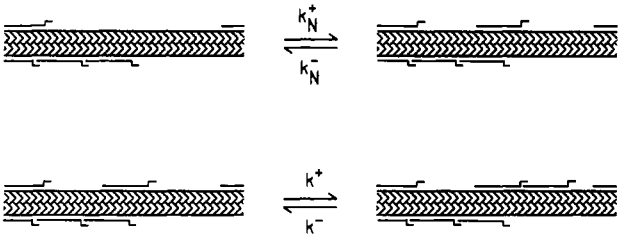

FIGURE 7: Reaction scheme of assembly of tropomyosin with actin filaments. Actin filament subunits are represented by chevrons. Tropomyosin molecules are presented by lines along the actin filaments. (Top) Binding of tropomyosin to an isolated binding site on an actin filament. (Bottom) Binding of tropomyosin to a contiguous binding site on an actin filament.

According to this model the time course of assembly of tropomyosin with actin filaments depends on the rates of two reactions, namely association or dissociation of a single tropomyosin molecule (rate constants k_N^+, k_N^- (see Figure 7)) and association or dissociation of contiguous tropomyosin molecules (rate constants k^+, k^-).

An equilibrium binding curve measured by light scattering and fluorescence is displayed in Figure 2. Below 0.9 μM total tropomyosin, which is equivalent to about 517 μM polymeric actin, the concentration of bound tropomyosin increases linearly with the total tropomyosin concentration. The binding curves of tropomyosin to actin filaments measured at higher temperatures reveal a sigmoidal shape indicating cooperative binding (Wegner, 1979). In the present experiments no sigmoidal shape can be observed because contiguous binding of tropomyosin is irreversible (Wegner & Ruhnau, 1988). The calculated curve of irreversible binding depicted in Figure 2 fits the experimental data within the limits of experimental error. Since contiguous binding is irreversible, the rate constant of dissociation of tropomyosin from an actin-bound tropomyosin cluster is set equal to zero ($k^- = 0$). Kinetic rate equations for this model of assembly of tropomyosin with actin filaments are derived in the Appendix.

Evaluation of the Experimental Data. Good agreement between calculations and the measured time course of assembly of tropomyosin with actin filaments is obtained if isolatedly bound and free tropomyosin are assumed to occur in equilibrium concentrations (see Appendix, eq 8). This fast preequilibrium between free and bound tropomyosin is achieved if dissociation of isolated tropomyosin is considerably faster than transformation of isolated tropomyosin into a tropomyosin cluster by contiguous binding of a second tropomyosin molecule ($k_N^- > k^+ c_t$, Figure 7). Figures 4 and 5 illustrate the time courses calculated for an equilibrium constant of association of tropomyosin with an isolated binding site $K_N = k_N^+/k_N^- = 2.6 \times 10^4$ M^{-1} and a rate constant of binding of tropomyosin to a contiguous binding site $k^+ = 38 \times 10^6$ M^{-1} s^{-1}. Good agreement between measurements and calculations is also obtained when it is assumed that the rate of contiguous binding is larger and the equilibrium constant for binding of isolated tropomyosin lower (e.g., $k^+ = 87 \times 10^7$ M^{-1} s^{-1}, $K_N = 5 \times 10^3$ M^{-1}). It is hardly conceivable, however, that the rate constant of contiguous binding k^+ is considerably larger than this value because a higher value would exceed the rate of a diffusion-controlled association reaction. It is not possible to find a satisfactory correspondence between measurements and calculations using a value of k^+ below 38×10^6 M^{-1} s^{-1} and an equilibrium constant K_N for binding of tropomyosin to isolated binding sites above 2.6×10^4 M^{-1}. The evaluation of the results indicate a low affinity of tropomyosin for isolated binding sites ($K_N \leq 2.6 \times 10^4$ M^{-1}). Because of the low affinity, only a minor amount of tropomyosin is bound to actin

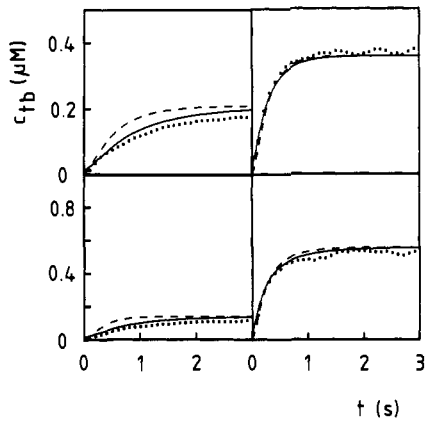

FIGURE 8: Comparison of two models of tropomyosin actin assembly with experimental data: c_{tb}, concentration of actin-bound tropomyosin; – – –, isolatedly bound tropomyosin was assumed to dissociate from actin filaments slowly (rate constant $k_N^- \approx 0$ (numerical integration of eqs 2–5 and 7)). —, a fast preequilibrium between free and isolatedly bound tropomyosin exists (numerical integration of eqs 3–5 and 7). (Top panels) 2.5 μM actin filaments. Tropomyosin concentrations: left 0.3 μM, right 0.8 μM. (Bottom panels) 5 μM actin filaments. Tropomyosin concentrations: left 0.2 μM, right 0.8 μM.

filaments in the fast preequilibrium between free and isolated tropomyosin (see eq 8). Therefore, a fast initial fluorescence increase brought about by binding of tropomyosin to isolated binding sites is expected to be small. For this reason and also because of the time resolution of the fluorescence stopped-flow device, a fast initial fluorescence jump could not be observed.

The time course of assembly was also calculated for the limiting case where dissociation of isolated tropomyosin from actin filaments is slow ($k_N^- \approx 0$). This situation is opposite to fast preequilibrium between free and isolated tropomyosin. The fit to the measured time course of assembly was poor (Figure 8).

Discussion

The time course of formation of tropomyosin actin filaments can be explained by a simple assembly model in which single tropomyosin molecules bind to isolated binding sites on actin filaments. Further tropomyosin molecules can bind adjacently to actin-bound tropomyosin to generate clusters of contiguous tropomyosin molecules. Good agreement of this model with the measured time course of assembly is obtained if one assumes a fast preequilibrium between free and isolatedly bound tropomyosin. Tropomyosin binds to actin filaments in a highly cooperative manner (Wegner, 1979, 1980; Walsh & Wegner, 1980), i.e., the affinity of tropomyosin for isolated binding sites is considerably lower than that for contiguous binding sites. The ratio between the affinities has been estimated to be 100-fold or 1000-fold (Wegner, 1979). The proposed assembly mechanism is in agreement with a highly cooperative binding reaction. In the postulated fast preequilibrium tropomyosin binds to isolated sites on actin filaments with low affinity ($K_N \approx 10^3$–10^4 M^{-1}). Irreversible high-affinity binding of isolated tropomyosin was shown not to be in agreement with the observed time course of tropomyosin actin assembly (Figure 8). Under the experimental conditions contiguous binding of tropomyosin is practically irreversible. Thus, the equilibrium constant K for contiguous binding is appreciably larger than the reciprocal of the free tropomyosin concentrations in our experiments ($K > 1/c_t \approx 10^7$ M^{-1}).

The rate of contiguous binding of tropomyosin has been investigated previously (Wegner & Ruhnau, 1988). In this investigation the decrease of the rate of actin polymerization brought about by tropomyosin, which binds near the ends of actin filaments, was analyzed in terms of rate of contiguous binding. At high monomeric actin concentrations and low tropomyosin concentrations, actin polymerization was not retarded by tropomyosin because actin polymerization was faster than contiguous binding of tropomyosin near the ends of actin filaments. Conversely, at low actin monomer concentrations and high tropomyosin concentrations, the rate of elongation of actin filaments was decreased because contiguous binding of tropomyosin near the ends of actin filaments was faster than that of actin monomers. A quantitative analysis of contiguous binding of tropomyosin along actin filaments gave rate constants of 2.5×10^6 to 4×10^6 M^{-1} s^{-1} (Wegner & Ruhnau, 1988). This assay yielded the rate of contiguous binding of tropomyosin toward the barbed ends of actin filaments because actin polymerization at the pointed ends is so slow (Pollard & Mooseker, 1981; Selve & Wegner, 1986) that it could not be observed simultaneously with polymerization at the barbed ends. In the measurements reported in this paper, contiguous binding at tropomyosin clusters both toward the barbed and the pointed ends is observed. The apparent rate of contiguous binding is thus the sum of the rates of association at both ends of clusters. This may explain the higher rate constant reported here ($>38 \times 10^6$ M^{-1} s^{-1}) compared to the rate constant determined previously (2.5×10^6 to 4×10^6 M^{-1} s^{-1}). Taking this effect into account brings the two rates within less than an order of magnitude, a difference which may not be significant. It is, however, also possible that the assumptions on which the evaluations of the two experiments are based require refinement or modification to account for the discrepancy.

Actin-bound tropomyosin clusters are formed by low-affinity binding of isolated tropomyosin and subsequent high-affinity binding of contiguous tropomyosin along actin filaments. The first step of this assembly process is not favored. Thus, the first step of formation of tropomyosin clusters can be considered as a nucleation, and the subsequent contiguous binding as growth. In many assembly processes that consist of nucleation and growth, an initial lag phase of assembly is observed at sufficiently low concentrations. For instance, polymerization of actin monomers at low concentrations is initially slow because spontaneous formation of short actin filaments from monomers is slow. As soon as these nuclei for actin polymerization have been formed, monomers polymerize rapidly onto the nuclei, leading to an increased rate of incorporation of monomers into filaments (Oosawa & Kasai, 1962). In the case of assembly of tropomyosin with actin filaments, no initial lag phase of binding of tropomyosin to actin can be observed (Figures 4 and 5). The reason for this lack of a slow initial assembly reaction rests on the great number of nucleation sites along actin filaments. The slow rate of formation of tropomyosin clusters is compensated by the large number of sites where clusters can start forming. A similar disappearance of the lag phase is observed in actin polymerization at high concentrations (Matsudaira et al., 1987).

When two tropomyosin clusters grow together on an actin filament, usually a small gap of actin filament subunits is expected to remain free of tropomyosin because in most cases two clusters are not separated by an integral multiple of seven subunits. On the basis of the evaluated equilibrium and rate constants ($K_N = 2.6 \times 10^4$ to 5×10^3 M^{-1}, $k^+ = 38 \times 10^6$ to 87×10^6 M^{-1} s^{-1}), one can calculate that at the end of the assembly reaction, on average every 50 actin filament subunits, a gap too small for insertion of tropomyosin occurs. If, however, tropomyosin actin filaments are formed by simultaneous

polymerization of actin and assembly of tropomyosin with growing actin filaments, then small gaps are expected not to arise because presumably all tropomyosin molecules bind consecutively and contiguously near the end of the polymerizing actin filament (Ruhnau & Wegner, 1988). An observation which can be taken as experimental evidence that the length of contiguously bound tropomyosin strands along actin filaments depends on the mode of formation of tropomyosin–actin filaments has been provided by Tanaka (1972). He found that tropomyosin which associated with polymerizing actin filaments was bound to actin filaments more strongly than tropomyosin which was added to polymerized actin filaments. Long contiguous strands of tropomyosin bind to actin filaments more strongly than short strands because in the long contiguous strands more end to end contacts between tropomyosin molecules occur.

The mode of formation of tropomyosin–actin filaments and the occurrence of small gaps could be of biological importance. It is known that α-actinin and filamin compete for binding to actin filaments with tropomyosin (Drabikowski et al., 1968; Maruyama et al., 1978). The number of attachment sites of α-actinin along actin filaments could be regulated by the number of small gaps and, therefore, may depend on the mode of assembly of tropomyosin with actin filaments. Tropomyosin has been reported to stabilize actin filaments against fragmentation by severing proteins, such as severin or gelsolin (Hinssen, 1981; Bernstein & Bamburg, 1982; Fattoum et al., 1983; Bonder & Mooseker, 1983; Ishikawa et al., 1989). It is conceivable that the number of fragmentation sites along actin filaments can be modulated by changing the number of small gaps that are not covered by tropomyosin.

Appendix

Kinetic Rate Equations for Binding of Tropomyosin to Actin Filaments. During the assembly process the concentrations of free tropomyosin and of isolatedly and contiguously bound tropomyosin change. For a quantitative description of this assembly process, kinetic rate equations for these concentrations have to be derived.

(a) Isolatedly bound tropomyosin (c_{t1}) is formed by association of free tropomyosin (c_t) with an appropriate binding site on an actin filament and disappears by dissociation from actin filaments or is transformed into a cluster of tropomyosin molecules by contiguous binding of a second tropomyosin molecule (Figure 7).

$$\frac{dc_{t1}}{dt} = k_N^+ c_t \sum((n-8)l_n) - k_N^- c_{t1} - k^+ c_t c_{t1} p = k_N^+ c_t \sum(nl_n) - k_N^+ c_t (8\sum l_n) - k_N^- c_{t1} - k^+ c_t c_{t1} p \quad (2)$$

l_n is the concentration of gaps containing n filament subunits free of tropomyosin in one strand of the double-helical actin filament. Only gaps that contain nine or more subunits can bind isolated tropomyosin. The number of binding sites in a gap is $n - 8$ (see Figure 7). p is the probability that an adjacent gap is sufficiently large to bind a tropomyosin molecule contiguously, i.e., seven or more subunits.

(b) The concentration of actin filament subunits free of tropomyosin changes by isolated binding of tropomyosin, by dissociation of isolated tropomyosin, and by contiguous binding of tropomyosin to isolated tropomyosin or to a tropomyosin cluster.

$$\frac{d\sum(nl_n)}{dt} = -7k_N^+ c_t \sum((n-8)l_n) + 7k_N^- c_{t1} - 7k^+ c_t c_{t1} p - 7k^+ c_t c_{cl} \quad (3)$$

c_{cl} is the concentration of clusters of contiguously bound tropomyosin molecules.

(c) Clusters containing two or more contiguously bound tropomyosin molecules are formed by binding of tropomyosin adjacently to isolated tropomyosin and disappear by coalescence of two clusters.

$$\frac{dc_{cl}}{dt} = k^+ c_t c_{t1} p - k^+ c_t c_{cl} q \quad (4)$$

q is the probability that following contiguous binding of a tropomyosin molecule the remaining gap is less than seven actin filament subunits long. In that case, two clusters separated by this small gap can be considered to have grown together as additional contiguous tropomyosin molecules cannot be inserted into the gap.

(d) The concentration of actin filament subunits c_{sg} that cannot be covered by tropomyosin because they are localized in small gaps containing less than six subunits increases by coalescence of tropomyosin clusters.

$$\frac{dc_{sg}}{dt} = 3k^+ c_t c_{cl} q \quad (5)$$

The factor of 3 is the average number of actin subunits occurring in small gaps ($(\sum n)/7$, $0 < n < 7$).

(e) The concentration of gaps $\sum l_n$ is equal to the concentration of isolatedly bound tropomyosin molecules c_{t1} and of tropomyosin clusters c_{cl} as each tropomyosin molecule or tropomyosin cluster is separated from the next bound tropomyosin by a gap.

$$\sum l_n = c_{t1} + c_{cl} \quad (6)$$

(f) The concentration of free tropomyosin c_t changes due to binding and dissociation of isolated tropomyosin molecules (c_{t1}), due to binding of tropomyosin contiguously to isolated tropomyosin and due to expansion of existing tropomyosin clusters.

$$\frac{dc_t}{dt} = -k_N^+ c_t \sum((n-8)l_n) + k_N^- c_{t1} - k^+ c_t c_{t1} p - k^+ c_t c_{cl} = 1/7 \frac{d\sum(nl_n)}{dt} \quad (7)$$

In the limiting case free tropomyosin occurs in equilibrium concentration with isolatedly bound tropomyosin molecules. This fast preequilibrium is achieved, if dissociation of isolated tropomyosin is considerably faster than transformation of isolated tropomyosin into a tropomyosin cluster by contiguous binding of a second tropomyosin molecule ($k_N^- > k^+ c_t$). Under this condition the set of kinetic rate equations can be simplified. The concentration of isolated tropomyosin c_{t1} can be easily calculated as a function of the free tropomyosin concentration c_t:

$$K_N = \frac{c_{t1}}{c_t \sum((n-8)l_n)} = \frac{c_{t1}}{c_t(\sum(nl_n) - 8\sum l_n)} \quad (8)$$

The only unknown quantities in eqs 2–8 are the probabilities p and q. The probability p that a gap adjacent to an isolated tropomyosin contains seven or more actin filament subunits can be calculated if the length distribution of gaps is known. An estimate of the length distribution of gaps can be obtained on the basis of the following consideration: As the assembly of tropomyosin with actin filaments is a highly cooperative process, only a few tropomyosin clusters are formed along actin filaments. When these clusters grow together, small gaps remain. The length of these gaps (=shifts) ranges from one

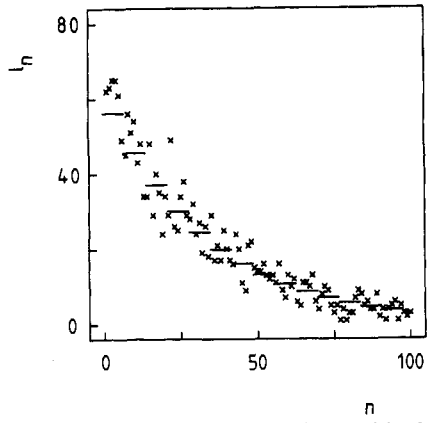

FIGURE 9: Length distribution of gaps calculated by Monte Carlo simulation (×) and using eqs 9, 10, and 12 (—): n, number of adjacent filament subunits not covered by tropomyosin; l_n, number of gaps of the length n. In the Monte Carlo calculation assembly of 100 filaments containing 1000 subunits was simulated. In the represented length distribution of gaps, 30% of filament subunits were covered by tropomyosin. Rate constants: $k_N^+ = 2.6 \times 10^6$ M^{-1} s^{-1}; $k_N^- = 100$ s^{-1}; $k^+ = 38 \times 10^6$ M^{-1} s^{-1}. Free tropomyosin concentration was 0.5 μM.

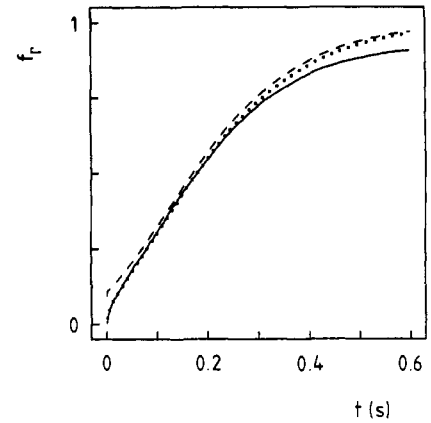

FIGURE 10: Monte Carlo simulation and calculation using eqs 2–13: fr, fraction of actin filament subunits covered with tropomyosin; —, the assembly of 100 filaments containing 1000 subunits was simulated by a Monte Carlo calculation. Rate constants: $k_N^+ = 2.6 \times 10^6$ M^{-1} s^{-1}; $k_N^- = 100$ s^{-1}; $k^+ = 38 \times 10^6$ M^{-1} s^{-1}. Free tropomyosin concentration was 0.5 μM. ···, calculation by integration of eqs 2–5 and 7 using the same rate constants and concentrations as for the Monte Carlo simulation. – –, calculation by integration of eqs 3–5 and 7, thereby assuming a fast preequilibrium between free and isolatedly bound tropomyosin: $K_N = k_N^+/k_N^- = 2.6 \times 10^4$ M^{-1}.

to six actin filament subunits. It is a reasonable assumption that all possible shifts occur with the same probability since the tropomyosin clusters are formed essentially independently from each other. Thus

$$l_0 = l_1 = ... = l_6 \tag{9}$$

Because of the independent formation of tropomyosin clusters the concentrations of gaps which contain the same number (m) of binding sites for tropomyosin molecules but differ by the shift s can be assumed to occur with the same probability.

$$l_{7m+0} = l_{7m+1} = ... = l_{7m+6} = l_{7m+s} \tag{10}$$

The length distribution of gaps containing different numbers m of binding sites can be assumed to be a geometric series since new gaps are formed by random insertion of tropomyosin into a gap.

$$l_{7m+n} = l_n \alpha^m \tag{11}$$

where α is a constant. Using eq 10 and 11, the probability p can be calculated to be

$$p = \frac{\sum l_n - (l_0 + l_1 + l_2 + l_3 + l_4 + l_5 + l_6)}{\sum l_n} = 1 + \frac{7\sum l_n}{\sum (n l_n) + 4\sum l_n} \tag{12}$$

In deriving eq 12 a number of approximations has been made. These approximations can be justified by comparison of the assumed length distribution of gaps with that obtained by Monte Carlo calculations (Epstein, 1979). The length distributions of gaps calculated by both methods are depicted in Figure 9.

The second quantity necessary for solving eq 2–8 is the probability q that following contiguous binding of a tropomyosin the remaining gap is less than seven actin filament subunits long (probability $1 - p$) and that an irreversibly bound tropomyosin cluster is localized beyond the gap (probability $c_{cl}/(c_{cl} + c_{tl})$). Thus

$$q = (1 - p) \frac{c_{cl}}{c_{cl} + c_{tl}} \tag{13}$$

Figure 10 illustrates that for a realistic set of rate constants the solutions of the kinetic equations and Monte Carlo simulations are similar, suggesting that the approximations are valid.

The time course of the concentration of bound tropomyosin c_{tb} was calculated as the difference between the total (c_{ttot}) and the free (c_t) tropomyosin concentration:

$$c_{tb} = c_{ttot} - c_t \tag{14}$$

In the case of a fast preequilibrium between free and isolatedly bound tropomyosin the time course of bound tropomyosin was calculated by numerical integration of eqs 3–5 and 7, thereby using eqs 6, 8, and 12–14. Other curves were calculated by integration of eqs 2–5 and 7, thereby using eqs 6 and 12–14.

REFERENCES

Bailey, K. (1948) *Biochem. J. 43*, 271–279.
Bernstein, B. W., & Bamburg, J. R. (1982) *Cell Motil. 2*, 1–8.
Berthet-Colominas, C., Bois, J. M., Cuillel, M., Sedita, J., & Vachette, P. (1984) *Rev. Phys. Appl. 190*, 769–772.
Bonder, E. M., & Mooseker, M. S. (1983) *J. Cell Biol. 96*, 1097–1107.
Boulin, C., Kempf, R., Koch, M. H. J., & McLaughlin, S. M. (1986) *Nucl. Instrum. Methods Phys. Res. A249*, 399–407.
Boulin, C., Kempf, R., Gabriel, A., & Koch, M. H. J. (1988) *Nucl. Instrum. Methods Phys. Res. A269*, 312–320.
Bremel, R. D., & Weber, A. (1972) *Nature, New Biol. 238*, 97–101.
Bretscher, A., & Weber, K. (1978) *FEBS Lett. 85*, 145–148.
Casper, D. L. D., Cohen, C., & Longley, W. (1969) *J. Mol. Biol. 41*, 87–107.
Clark, I. D., & Burtnick, L. D. (1988) *Arch. Biochem. Biophys. 260*, 595–600.
Cohen, I., & Cohen, C. (1972) *J. Mol. Biol. 68*, 383–387.
Cotê, G., Lewis, W. G., & Smillie, L. B. (1978) *FEBS Lett. 91*, 237–241.
Cotê, G. P., & Smillie, L. B. (1981) *J. Biol. Chem. 256*, 7257–7261.
Der Terrossian, E., Fuller, S. D., Stewart, M., & Weeds, A. G. (1981) *J. Mol. Biol. 153*, 147–167.
Drabikowski, W., Nonomura, Y., & Maruyama, K. (1968) *J. Biochem. (Tokyo) 63*, 761–766.
Ebashi, S., Endo, M., & Ohtsuki, I. (1969) *Q. Rev. Biophys. 2*, 351–384.

Eisenberg, E., & Kielley, W. W. (1974) *J. Biol. Chem. 249*, 4742–4748.
Elzinga, M., Collins, J. H., Kuehl, W. M., & Adelstein, R. S. (1973) *Proc. Natl. Acad. Sci. U.S.A. 70*, 2687–2691.
Epstein, I. R. (1979) *Biopolymers 18*, 2037–2050.
Fattoum, A., Hartwig, J. H., & Stossel, T. P. (1983) *Biochemistry 22*, 1187–1193.
Fine, R. E., Blitz, A. L., Hitchcock, S. E., & Kaminer, B. (1973) *Nature, New Biol. 245*, 182–186.
Gabriel, A., & Dauvergne, F. (1982) *Nucl. Instrum. Methods 201*, 223–224.
Giometti, C. S., & Anderson, N. L. (1984) *J. Biol. Chem. 259*, 14113–14120.
Hartshorne, D. J., & Pyun, H. Y. (1971) *Biochim. Biophys. Acta 229*, 698–711.
Hinssen, H. (1981) *Eur. J. Cell Biol. 23*, 234–240.
Hitchcock-DeGregori, S. E., Sampath, P., & Pollard, T. D. (1988) *Biochemistry 27*, 9182–9185.
Hodges, R. S., Sodek, J., Smillie, L. B., & Jurasek, L. (1972) *Cold Spring Harbor Symp. Quant. Biol. 37*, 299–310.
Hosoya, M., Miyazaki, J.-I., & Hirabayashi, T. (1989) *J. Biochem. (Tokyo) 105*, 712–717.
Huxley, H. E., & Brown, W. (1967) *J. Mol. Biol. 30*, 383–434.
Ishikawa, R., Yamashiro, S., & Matsumara, F. (1989) *J. Biol. Chem. 264*, 7490–7497.
Jahnke, U., & Heilmeyer, L. M. G. (1983) *Eur. J. Biochem. 133*, 591–597.
Keiser, T., & Wegner, A. (1985) *FEBS Lett. 187*, 76–80.
Kobayashi, R., Tawata, M., Mace, M. L., Bradley, W. A., & Field, J. B. (1982) *Biochim. Biophys. Acta 702*, 220–232.
Koch, M. H. J., & Bordas, J. (1983) *Nucl. Instrum. Methods Phys. Rev. A208*, 461–469.
Laki, K., Maruyama, K., & Kominz, D. R. (1962) *Arch. Biochem. Biophys. 98*, 323–330.
Lal, A. A., & Korn, E. D. (1986) *Biochemistry 25*, 1154–1158.
Lazarides, E. (1976) *J. Supramol. Struct. 5*, 531–563.
Liu, H., & Bretscher, A. (1989) *Proc. Natl. Acad. Sci. U.S.A. 86*, 90–93.
Lowry, O. H., Rosebrough, N. J., Farr, A. L., & Randall, R. (1951) *J. Biol. Chem. 193*, 265–275.
Martonosi, A. (1962) *J. Biol. Chem. 237*, 2795–2805.
Maruyama, K., & Ohashi, K. (1978) *J. Biochem. (Tokyo) 84*, 1017–1019.
Matsudaira, P., Bordas, J., & Koch, M. H. J. (1987) *Proc. Natl. Acad. Sci. U.S.A. 84*, 3151–3155.
McLachlan, A. D., Stewart, M., & Smillie, L. B. (1975) *J. Mol. Biol. 98*, 281–291.
O'Brien, E. J., Bennett, P. M., & Hanson, J. (1971) *Philos. Trans. R. Soc. London B 261*, 201–208.
Oosawa, F., & Kasai, M. (1962) *J. Mol. Biol. 4*, 10–21.
Parry, D. A. D. (1975) *J. Mol. Biol. 98*, 519–535.
Pollard, T. D., & Mooseker, M. S. (1981) *J. Cell Biol. 88*, 654–659.
Prendergast, F. G., Meyer, M., Carlson, G. L., Iida, S., & Potter, J. D. (1983) *J. Biol. Chem. 258*, 7541–7544.
Rees, M. K., & Young, M. (1967) *J. Biol. Chem. 242*, 4449–4458.
Sayers, Z., Koch, M. H. J., Bordas, J., & LIndberg, U. (1985) *Eur. Biophys. J. 13*, 99–108.
Schloss, J. A., & Goldman, R. D. (1980) *J. Cell Biol. 87*, 633–642.
Selve, N., & Wegner, A. (1986) *Eur. J. Biochem. 160*, 379–387.
Spudich, J. A., & Watt, S. (1971) *J. Biol. Chem. 246*, 4866–4871.
Spudich, J. A., Huxley, H. E., & Finch, J. T. (1972) *J. Mol. Biol. 72*, 619–632.
Szczesna, D., Borovikov, Y. S., Kakol, I., & Sobieszek, A. (1989) *Biol. Chem. Hoppe-Seyler 370*, 399–407.
Tanaka, H. (1972) *Biochim. Biophys. Acta 278*, 556–566.
Tanaka, H., & Oosawa, F. (1971) *Biochim. Biophys. Acta 253*, 274–283.
Tanaka, H., & Hatano, S. (1972) *Biochim. Biophys. Acta 257*, 445–451.
Walsh, T. P., & Wegner, A. (1980) *Biochim. Biophys. Acta 626*, 79–87.
Wegner, A. (1976) *J. Mol. Biol. 108*, 139–150.
Wegner, A. (1979) *J. Mol. Biol. 131*, 839–853.
Wegner, A. (1980) *FEBS Lett. 119*, 245–248.
Wegner, A. (1982) *J. Mol. Biol. 161*, 217–227.
Wegner, A., & Ruhnau, K. (1988) *Biochemistry 27*, 6994–7000.
Yang, Y. Z., Korn, E. D., & Eisenberg, E. (1979) *J. Biol. Chem. 254*, 7137–7140.
Zeece, M. G., Robson, R. M., & Bechtel, P. J. (1979) *Biochim. Biophys. Acta 581*, 365–370.